Environ Sci Pollut Res (2016) 23:25105–25113
DOI 10.1007/s11356-016-7617-x

RESEARCH ARTICLE

Alternative dry separation of PM_{10} from soils for characterization by kinetic extraction: example of new Caledonian mining soils

Camille Pasquet[1] · Peggy Gunkel-Grillon[1] · Christine Laporte-Magoni[1] · Arnaud Serres[1] · Thomas Quiniou[1] · François Rocca[1] · Fabrice Monna[2] · Remi Losno[3] · Folkert van Oort[4] · Carmela Chateau[5]

Received: 9 June 2016 / Accepted: 7 September 2016 / Published online: 27 September 2016

Abstract A simple new device for dry separation of fine particulate matter from bulk soil samples is presented here. It consists of a stainless steel tube along which a nitrogen flow is imposed, resulting in the displacement of particles. Taking into account particle transport, fluid mechanics, and soil sample composition, a tube 6-m long, with a 0.04-m diameter, was found best adapted for PM_{10} separation. The device rapidly produced several milligrams of particulate matter, on which chemical extractions with EDTA were subsequently performed to study the kinetic parameters of extractable metals. New Caledonian mining soils were chosen here, as a case-study. Although the easily extracted metal pool represents only 0.5–6.4 % of the total metal content for the elements studied (Ni, Co, Mn), the total concentrations are extremely high. This pool is therefore far from negligible, and can be troublesome in the environment. This dry technique for fine particle separation from bulk parent soil eliminates the metal-leaching risks inherent in wet filtration and should therefore ensure safe assessment of environmental quality in fine-textured, metal-contaminated soils.

Keywords Dry separation · PM_{10} · Dust · Physical modeling · EDTA · Kinetic extraction · Ultramafic soil · Trace metals

Responsible editor: Philippe Garrigues

Electronic supplementary material The online version of this article (doi:10.1007/s11356-016-7617-x) contains supplementary material, which is available to authorized users.

✉ Camille Pasquet
camille.pasquet@univ-nc.nc

[1] PPME, Université de la Nouvelle-Calédonie, BP R4, 98851 Nouméa Cedex, Nouvelle-Calédonie, France

[2] UMR 6298, ArTeHis, Université de Bourgogne – Franche Comté - CNRS-Culture, 6 bd Gabriel, Bat. Gabriel, 21000 Dijon, France

[3] Institut de Physique du Globe de Paris (IPGP), Sorbonne Paris Cité, UMR CNRS 7154, Université Paris Diderot, 1 rue Jussieu, 75013 Paris, France

[4] UMR 1402 Ecosys, INRA-AgroParisTech, pôle Ecotoxicologie, Centre de Versailles-Grignon, RD 10, 78026 Versailles Cedex, France

[5] Université de Bourgogne-Franche Comté, UFR SVTE, 6 bd Gabriel, Bat. Gabriel, 21000 Dijon, France

Introduction

Mining processes emit small airborne particles enriched in trace metals (Sinha and Banerjee 1997; Chakraborty et al. 2002), which may adversely affect air quality. The total suspended particle fraction is defined as particles smaller than 100 μm. The smallest particles can easily penetrate the human respiratory system, causing respiratory dysfunction (e.g., asthma or bronchitis), cardiovascular diseases, cancer, kidney damage, etc. (Järup 2003; Kampa and Castanas 2008). As a consequence, the chemical characterization of PM_{10} (particulate matter in which 50 % of the particles are below 10 μm in diameter; Janssen et al. 1998) is of great interest for health and ecotoxicological risk evaluation (Harrison et al. 1997; Ragosta et al. 2006; Sánchez de la Campa et al. 2007).

In New Caledonia, where mining is not only a major economic activity but also a potential health hazard, it is important to quantify trace metal bioavailability of PM_{10} emitted by mining soils. Potentially deleterious effects can be assessed by studying the kinetic extraction behavior of trace metals, hypothesized to mimic their bioavailability in the environment (Gutzman and Langford 1993; Bermond et al. 1998; Lo and Yang 1999). Ethylenediaminetetraacetic acid (EDTA) can be

used as a strong non-specific chelating agent (Bermond et al. 1998; Peters 1999; Labanowski et al. 2008; Jalali and Tabar 2013; Camizuli et al. 2014), to extract metals associated with carbonates, organic matter, oxides, or clay minerals (Lo and Yang 1999; Manouchehri et al. 2006). Kinetic extraction behaviors are modeled by the sum of first-order reactions, typically two (Gutzman and Langford 1993; Fangueiro et al. 2005; Bermond et al. 2005; Labanowski et al. 2008; Camizuli et al. 2014). The first pool corresponds to the easily extractable metals, while the second corresponds to the less readily extractable metals, assumed to be only potentially available (Fangueiro et al. 2005; Bermond et al. 2005). The remaining fraction is the EDTA non-extractable metal pool. Although powerful and informative, this kinetic extraction approach requires a consistent amount of material (about 150 mg), which cannot easily be sampled outdoors with conventional air pumps, size cutoff inlets (cascade or impactors), and filters (Harrison et al. 1997; Tasić et al. 2006; Geagea et al. 2008). Such conventional samplers only collect few milligrams of atmospheric particles. Wet separation techniques of PM_{10} fractions, including wet sieving (Ljung et al. 2008; Luo et al. 2011), wet sedimentation (Ajmone-Marsan et al. 2008; Madrid et al. 2008; Boisa et al. 2014), and elutriation (Webber et al. 2008) in the laboratory, are unfortunately not better options. Although these techniques can isolate a much larger amount of fine particulate matter, a non-negligible fraction of elements may be leached by wet separation, resulting in a distorted chemical characterization of the particles isolated (Morselli et al. 2003). As summarized by Gill et al. (2006), several dry separation techniques have also been designed for the laboratory. They are based on gas dispersion and fluidized bed technology (Chow et al. 1994; Carvacho et al. 2002), gravitation (Singer et al. 2003) or mechanical dispersion/agitation (Gill et al. 1999; Lafon et al. 2014). However, almost all of them use filters, which can quickly become saturated, thus reducing their collection capability. Filters are also prone to being affected by external pollution, which is problematic given the low amount of material collected (Jones et al. 2001; Greenwell et al. 2002). Ideally, particle separation should therefore be performed in dry conditions, without filters. To our knowledge, only Goossens (2012) has proposed such a technique, including a first step with a dust separator to remove the coarser particles and a second step with an inclined elutriator and a vacuum cleaner to collect the finest particles. However, using a bag to protect the device from particles and to collect the fine sediment can affect PM_{10} chemical characterization, through sample loss and/or external pollution.

The point here is to develop a new system allowing the collection of sufficient amounts of fine particles, by limiting the leaching of metal as much as possible either because of wet separation or external pollution due to filters. We thus propose a simple, new technique for separating fine particulate matter from bulk soils, in adequate amounts for further kinetic extraction. The aim is to mimic the effect of wind on soils, based on particle displacement along a tube, under a gas flow, where coarse particles are supposed to settle more rapidly than finer ones. The use of a simple 2D dynamic model, combined to fluid mechanics, is constructed to attempt in order to determine the tube geometry and operating conditions necessary to produce the targeted size fraction. The pertinence of the proposed model is then checked, using metal-enriched mining soils from New Caledonia, where Ni concentrations typically exceed 2 %. Such high values are of environmental concern, and the information provided by kinetic extraction of metals (Ni, Co, Mn) on the PM_{10} fraction can be used for environmental risk assessment.

Materials and methods

Soil sampling and preparation Four surface soil samples (~0–10 cm) were collected in the vicinity of two New Caledonian active mines: Poro-A and Poro-B, close to the Poro mine, on the southeast coast, and KNS-A and KNS-B, close to the KNS mine, in the southwest (Table 1). These soils have been frequently reworked by open-cast mining processes. They correspond to the B horizons of humid weathering profiles, and can be classified as Ferric Technosoils (IUSS Working Group WRB 2014). The samples were then dried at 35 °C, sieved at 2 mm, and quartered, to produce the $F_{<2mm}$ fraction. Their color was determined using a Munsell soil color chart after drying. This $F_{<2mm}$ soil fraction was then sieved again at 100 μm to produce a finer fraction, $F_{<100\mu m}$. About 2.5 g of $F_{<100\mu m}$ was placed at the entrance of the stainless steel separation tube, under a 1-bar nitrogen flow (~10^5 Pa), for a 60-s run, to collect an even smaller soil fraction, in a U-bend collector, at the end of the tube (Fig. 1). At that point, it is worth mentioning that negligible contamination from stainless steel is expected considering the extremely high concentrations in Ni, Mn, and Co of our treated samples. For less enriched soils, the potential contamination from stainless steel tube abrasion should be checked. The plastic U-bend collector is encased and screwed into the tube; from which any leak is prevented by the use of a seal. The turbulent flow at the entrance of the tube lifts the particles, and the laminar flow then transports them along the tube. The tube geometry necessary to produce the targeted PM_{10} fraction will be discussed in detail later. Typically, 3 to 5 mg of PM_{10} was obtained by a pre-cleaned brush after one 60-s run, similar to values obtained using a filter unit. After each 60-s run, the tube was emptied and reloaded with new samples, until a sufficient amount of PM_{10} was collected. In order to prevent any health risk for technical operators, the use of a protective mask is recommended.

Table 1 Main physico-chemical characteristics of bulk Ferric Technosoils sieved at 2 mm, total metal content Q_{tot} and granulometric size distribution for $F_{<2mm}$ and $F_{<100\mu m}$ samples

Soil samples	Poro-A				Poro-B				KNS-A				KNS-B			
Coordinates (in WGS84) Long; Lat	165.692; −21.311				165.73; −21.305				164.811; −20.990				164.804; −20.977			
Color[a]	Strong brown (7.5YR 4/6)				Dark yellowish brown (10YR 4/4)				Yellowish brown (10YR 5/6)				Reddish yellow (7.5YR 6/6)			
pH	5.66				7.80				6.85				6.85			
C/N	30.3				nd				28.9				39.3			
OM (g kg^{-1})	1.44				0.77				4.79				2.85			
$CaCO_3$ (g kg^{-1})	3				4				2				<1			
CEC (cmol kg^{-1})	4.2				6.48				3.89				2.11			
$F_{<2mm}$ D50 in μm (span*)	365 (2.7)				198 (3.7)				64 (7.5)				29 (5.6)			
Q_{tot} in $F_{<2mm}$ (mg kg^{-1}) except Fe in % *w/w*	Ni	Co	Mn	Fe	Ni	Co	Mn	Fe	Ni	Co	Mn	Fe	Ni	Co	Mn	Fe
	18,100	629	2300	13	13,200	520	1130	7	20,200	581	3310	26.2	12,800	1410	5780	36.5
$F_{<100\mu m}$ D50 in μm (span*)	25 (*2.5*)				*37* (*2.0*)				*47* (*2.2*)				*25* (*3.2*)			
Q_{tot} in $F_{<100\mu m}$ (mg kg^{-1}) except Fe in % *w/w*	Ni	Co	Mn	Fe	Ni	Co	Mn	Fe	Ni	Co	Mn	Fe	Ni	Co	Mn	Fe
	23,600	1160	3530	21.2	17,900	898	2280	10.3	22,300	661	3780	29.2	14,400	1390	5270	37.6

nd non detected

[a] Munsell soil color chart

*Span is used to assess the width of the size distribution and calculated from (D90-D10)/D50

Physical and chemical characterization of soil fractions Particle size distribution was measured with a Mastersizer S2000 laser Particle Size Analyzer (Malvern®, UK), particle and water refractive indices of 2.9 and 1.33, stirred at 2100 rpm without ultrasound, for five measurement cycles of 20 s, using a general calculation model for irregular particles. The median diameter (D50) was used to characterize the central tendency of the size distribution. Dispersion of particle size (span) was evaluated by dividing the difference between the 90th and 10th percentiles by the D50 value. A mean specific mass of ρ = 2800 kg m^{-3} was measured by pycnometer. Mineralogical characterization was determined by x-ray diffraction (INEL CPS 120° Curved Position Sensitive Detector, $K_{\alpha Co}$).

Organic matter content (by loss-on-ignition at 550 °C), $CaCO_3$ content (by Bernard calcimeter); pH (in water medium with a 1:5, *v*/*v* ratio); C/N (by Thermo NA-2000 CHN analyzer), and cation exchange capacity (CEC) (using cobaltihexamine extraction), were determined on the $F_{<2mm}$ at the INRA national soil analysis laboratory, COFRAC certified, using standard AFNOR and ISO methods (AFNOR 2004; more details about quality control can be found at http://www5.lille.inra.fr/las). Total Fe, Co, Ni, and Mn concentrations were measured after total digestion by HNO_3, HCl, and HF of suprapure grade (ISO 14869–1) in the $F_{<2}$

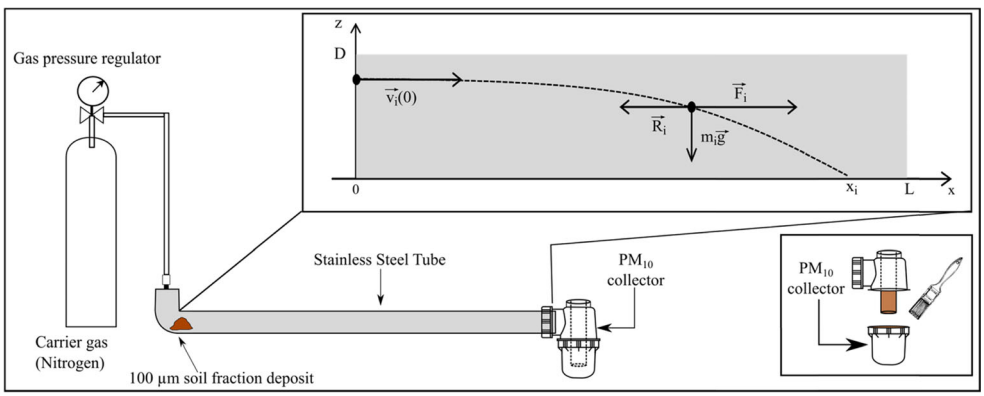

Fig. 1 *Bottom left* the device for fine particulate matter separation. *Bottom right* focus on the PM_{10} collector receptor during sample collection. *Top right* the dynamic model for particulate matter displacement in the tube; *L* for tube length, *D* for tube diameter, v_i the initial speed, R_i the air resistance to particle displacement, $m_i g$ the particulate weight, and F_i the force induced by the gas flow

$_{mm}$ and $F_{<100\mu m}$ fractions by the INRA national soil analysis laboratory, and, in the PM_{10} fraction, by ICP-AES at the Institut de Physique du Globe, Paris. A dozen blanks and certified reference materials (CRMs): PACS1, JSD1, JSD2 and BCSS1, were processed together with each batch of samples. Blank values were negligible for all elements measured. Data from CRMs differed by less than ±15 % from certified values.

Kinetic extractions Kinetic extractions of Ni, Co, and Mn were performed at pH = 6.5 on the PM_{10} fraction with 0.05 mol L^{-1} Na_2H_2-EDTA used as extractant. About 150 mg of PM_{10} material, precisely weighed, was mixed with 10 mL of extractant, and stirred with a 3D Polymax 1040 Heidolph. 200 μL of samples were collected at increasing times: $t \in$ [5, 10, 15, 20, 30, 45, 60, 90, 120, 150, 200, 250, 300, 500, 1440] min, after 1-min centrifugation at 4200 rpm. The solutions were adjusted to 5 mL with MilliQ water, without filtration. The Ni, Co, and Mn concentrations were measured at the Institut de Physique du Globe de Paris by ICP-AES, following the operating conditions mentioned above.

The kinetic extraction curves of Ni, Co, and Mn using EDTA were fitted using a two first-order reaction model:

$$Q(t) = Q_1\left(1-e^{-\lambda_1 t}\right) + Q_2\left(1-e^{-\lambda_2 t}\right) + \varepsilon_t \quad (1)$$

where $Q(t)$ is the amount of metal extracted per weight unit at time t, Q_1 is the readily extractable metal pool (labile pool) associated with the constant λ_1 (min^{-1}), Q_2 is the less labile pool associated with λ_2 (min^{-1}), while ε_t is the error (Fangueiro et al. 2005).

Data processing Non-linear regressions were performed using the nls package (Baty et al. 2015) for the free R software (R Development Core Team 2012). Graphics were generated using the ggplot2 package (Wickham 2009).

The 2D dynamic model

For modeling, particles composing the $F_{<100\mu m}$ fraction are assumed to be isolated, hard spheres of specific mass ρ. Any particle i is characterized by its diameter ϕ_i and its mass m_i (given a specific mass of ρ = 2800 kg m^{-3}, a particle with a typical diameter $\phi_i = 50$ μm possesses a mass of $m_i = 1.83 \times 10^{-10}$ kg). Its initial position at the entrance of the tube of length L and diameter D is ($x_i(0) = 0, z_i(0) = z_{0,i}$ with $0 < z_{0,i} < D$), while its speed is $\overrightarrow{v_i}(0) = v_{0,i}\overrightarrow{e_x}$ (Fig. 1). Along the trajectory, particles are subject to their weight, $m_i\overrightarrow{g}$, a force corresponding to the gas flow, $\overrightarrow{F_i} = F_i \times \overrightarrow{e_x}$, and to the resistance to particle displacement proportional to its speed, $\overrightarrow{R_i} = -\alpha_i \times \overrightarrow{v_i}$, with $\alpha_i = 3\phi_i$, and η the gas resistance. Introducing the new variable $\tau_i = \frac{m_i}{\alpha_i}$, the trajectory of the particle i is obtained according to the laws of motion:

$$\begin{cases} x_i(t) = \tau_i\left(v_{0,i} - \frac{F_i}{\alpha_i}\right)\left[1-\exp\left(-\frac{t}{\tau_i}\right)\right] + \frac{F_i}{\alpha_i}t \end{cases} \quad (2)$$

$$\begin{cases} z_i(t) = -g\tau_i^2\left[1-\exp\left(-\frac{t}{\tau_i}\right)\right] - g\tau_i t + z_{0,i} \end{cases} \quad (3)$$

For the N_2 gas flow, at pressure $P = 10^5$ Pa, and $\eta = 1.76 \times 10^{-5}$ Pa . s, the result is $\tau_i = 0.0221$ s. Considering the behavior of fluids in cylindrical geometries, the speed of the gas at the exit of the pressure regulator is around a few meters per second, which is also considered to be the initial speed of the particle $v_{0,i}$. In addition, a pressure drop, ΔP, of about 10–100 Pa appears at the exit of the regulator, imposing on the particle the force $F_i = \pi\left(\frac{\phi_i}{2}\right)^2 \Delta P$. Then, for a particle of diameter $\phi_i = 50$ μm and for $\Delta P = 50$ Pa, the ratio $\frac{F_i}{\alpha_i} = 11.8$ m. s^{-1}. From these results, the motion equations described by Eq. 2–3 can be simplified. As τ_i is small and the duration of the experiment is 60 s, the term $\exp\left(-\frac{t}{\tau_i}\right)$ can be neglected. As $v_{0,i}$ and $\frac{F_i}{\alpha_i}$ are within the same order of magnitude (a few meters per second), the term $\tau_i\left(v_{0,i} - \frac{F_i}{\alpha_i}\right)$ is negligible. Using these approximations, Eq. 2 and Eq. 3 become:

$$\begin{cases} x_i(t) \approx \frac{F_i}{\alpha_i}t \end{cases} \quad (4)$$

$$\{z_i(t) \approx -g\tau_i t + z_{0,i} \quad (5)$$

When a particle i exits from the tube at time t_{ex}, its position verifies $x_i(t_{ex}) > L$ and $z_i(t_{ex}) = 0$, so that the starting position of this particle must satisfy: $z_{0,i} > \frac{m_i g}{F_i}L$. Using an equiprobable distribution of initial positions, the probability for a particle i of size ϕ_i to exit the tube is given by the function, S(i), defined by:

$$S(\phi_i) = \frac{D - z_{0,1}}{D} = 1 - \frac{2}{3}\frac{g}{\Delta P} \times \frac{L}{D}\phi_i \quad (6)$$

Finally, the exit fraction $X(\phi_i)$ is obtained, considering an initial size distribution $E(\phi_i)$ at the entrance of the tube:

$$X(\phi_i) = S(\phi_i) \times E(\phi_i) \quad (7)$$

Results and discussion

Soil physico-chemical characteristics The four soils are moderately acid to slightly alkaline (5.7 ≤ pH ≤ 7.8). They are yellowish brown due to the presence of high amounts of

iron oxides and exhibit low OM values related to mining activities (Losfeld et al. 2015), as vegetation and topsoil were removed during mining process. They present low CEC values, typical for weathered ultramafic soils (Chesworth 2008), such as ferric technosoils (Table 1). The weathering of ultramafic rocks leads to the relative accumulation of metallic oxides, such as iron or manganese oxides, until 50 to 80 % of Fe_2O_3 in ferritic soil (Latham et al. 1978; Quantin et al. 1996). In the present study, soils are rich in iron oxides, with Fe_2O_3 amounting between 15 and 50 %. Metallic oxides generally have a zero point charge (ZPC) between pH 4–4.5 but the pH may rise up to 6–6.5 in oxide rich soils. As CEC by cobaltihexamine is performed at a pH close to the in situ soil conditions, the measured oxide charges are consequently low. The soils are predominantly composed of goethite (FeOOH) and to a lesser extent, lizardite ($Mg_3(Si_2O_5)(OH)_4$), hematite (Fe_2O_3), quartz (SiO_2) and antigorite ($(Mg,Fe)_3Si_2O_5(OH)_4$). Due to their mineralogy, the four $F_{<2mm}$ fractions present very high contents of Fe (7–37 %), Ni (1.3–2 %), Co (520–1410 mg kg^{-1}), and Mn (1130–5780 mg kg^{-1}) (Table 1), consistent with data from other mining soils in New Caledonia (Trescases 1973; Quantin et al. 2002). The fractions sieved at 100 μm ($F_{<100\mu m}$) exhibit similar metal contents, often slightly higher, as expected (e.g., Semlali et al. 2001). The particle size distribution of the $F_{<2mm}$ soil sample is variable, with D50 = 29–365 μm (Table 1), see supplementary information for particle size distribution curves.

Choice of tube geometry The 2D dynamic model, as defined by Eq. 6, was implemented in a calculator, in order to estimate the influence of the tube geometry (length L and diameter D) on the median size of the exit fraction. To test the model, a Gaussian distribution (mean c = 50 μm, standard deviation $\sigma = 2 \times 10^{-5}$) was chosen for the size distribution, $E(\phi_i)$, of the material to be processed. The results obtained by varying the values of the tube length L and its diameter D on the exit fraction are shown in Fig. 2. As the tube length increases, from 2 to 10 m (with constant diameter D = 0.04 m), the median diameter of collected particles decreases, from 44.5 to 11.5 μm (Fig. 2a). Furthermore, as the diameter decreases, from 0.9 to 0.1 m (with constant length L = 2 m), the median diameter of collected particles decreases, from 48.2 to 15 μm (Fig. 2b). These findings indicate that a long, narrow tube is required to isolate the desired PM_{10} fraction. If this model is applied to the case study soils, where the size distribution is not modeled, but measured, the optimal tube geometry is L = 6 m and D = 0.04 m, to obtain the targeted PM_{10} fraction. Figure 3 shows the size distribution for the Poro-B sample: (i) for $F_{<2mm}$, (ii) for $F_{<100\mu m}$, (iii) for the experimental PM_{10} fraction (with optimal tube geometry), and (iv) the theoretical PM_{10} fraction, according to the dynamic model (Eq. 7). The median diameter drops from about 200 μm for the $F_{<2mm}$ fraction, to about 35 μm for the $F_{<100\mu m}$ fraction, and to 11 μm for experimental PM_{10}, which is in good agreement with the theoretical predictions. Similar results for experimental PM_{10}, close to the targeted value of D50 ~ 10 μm, were obtained for all four samples (Table 2). Some slight differences are observed for the smallest diameters, which could have several possible causes (Fig. 3). The dynamic equations, which assume no interaction between hard spheres characterized by the same specific mass and an equiprobable distribution of initial positions, may be oversimplified. The dynamic model for particle separation is established for a gas medium, but particle size analysis was performed in water. Particles may aggregate and thus become too big to exit the tube. In water, however, most aggregates are likely to break down, particularly with the case-study soils, where organic matter does not play an aggregating role, and where mineral reactivity is low, as indicate by the very small CEC values (Huang et al. 2012). Finally, a non-negligible part of the smallest particles may be lost, because the end of the tube is open, which could explain the deficit observed in the smallest particles collected, in comparison with the theoretical model.

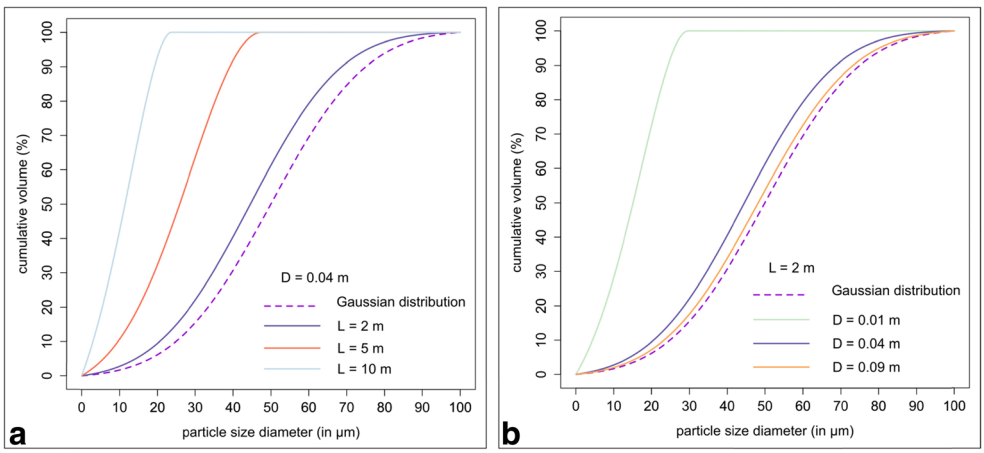

Fig. 2 Influence of tube length L and tube diameter D on particle size distribution after separation in the tube by **a** varying L and keeping D constant (D = 0.04 m), and **b** by varying D and keeping L constant (L = 2 m). The *dashed curve* corresponds to modeled Gaussian distribution (mean = 50 μm and standard deviation $\sigma = 2 \times 10^{-5}$ μm); other curves represent modeled particle size distribution of the material exiting the tube. Cumulative distributions are expressed in terms of particle volume, equivalent to cumulative mass

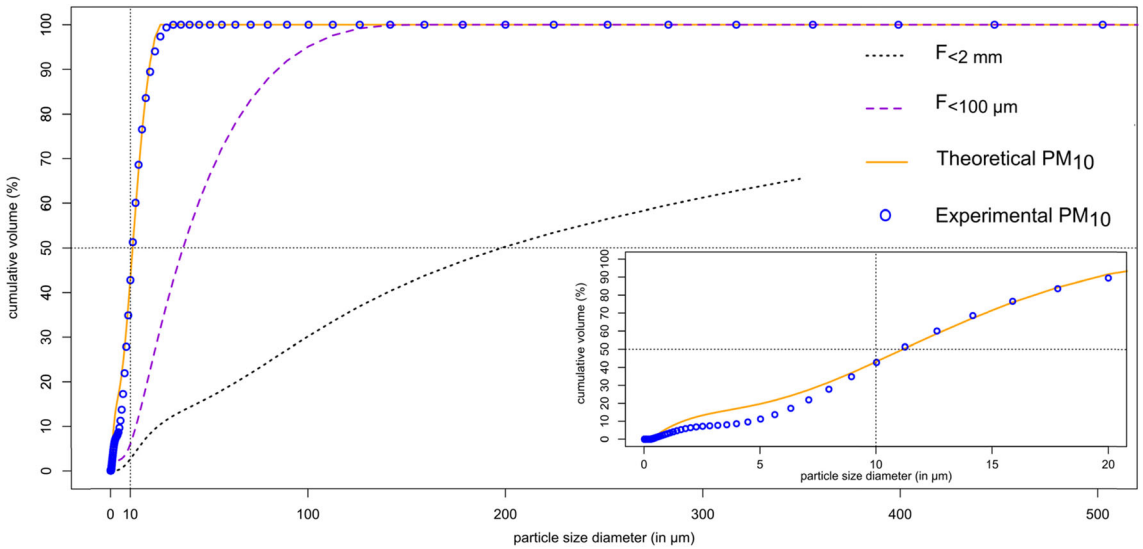

Fig. 3 Granulometric distributions of the Poro-B bulk soil ($F_{<2mm}$), the fraction sieved at 100 μm ($F_{<100\mu m}$), the experimental PM_{10} fraction separated in the tube, and theoretical expectations for particles at the exit with L = 6 m and D = 0.04 m. *Bottom right* a close up of experimental PM_{10} and theoretical expectations, with the *x*-axis reduced to 0–20 μm

The separation efficiency (SE) of the tube settings can also be estimated by calculating the ratio of the volume size distribution of the fraction collected at the exit of the tube $\phi(PM_{10})$, and that of the fraction placed at the entrance $\phi(F_{<100\mu m})$, as described by Goossens (2012):

$$SE = \frac{\phi(PM_{10})}{\phi\left(F_{<100\mu m}\right)} \quad (8)$$

Except for KNS-A, SE values equal to or above 1 were observed for particles up to 20 μm and then decreasing rapidly for coarser particles (Fig. 4). The maximum separation efficiency values varied between ~2 and 15, and were observed for particles between 5 and 10 μm, depending on the sample. The separation efficiency curves have similar shape of those obtained by Goossens (2012) Indeed, not only a poor separation efficiency for particles size between 0.1 and 5 μm, but also a maximum for particles between 5 and 10 μm, followed by a rapidly drop of the separation efficiency for coarser particles (above around 50 μm for Goossens (2012) and above 15–20 μm in this study) could be observed. In a general

Table 2 Granulometric size distribution and kinetic extraction parameters for separated PM_{10}

Soil samples	Poro-A			Poro-B			KNS-A			KNS-B		
D50 in μm (span*)	11 (*1.6*)			11 (*1.4*)			10 (*1.4*)			10 (*1.7*)		
Metal content	Ni	Co	Mn	Ni	Co	Mn	Ni	Co	Mn	Ni	Co	Mn
Q_{tot} (mg kg^{-1})	29,066	1077	4470	18,969	755	2222	22,187	615	3760	12,347	790	3720
Q_1 (mg kg^{-1})	360.0	17.8	99.6	709.0	22.1	60.5	458.0	30.7	182.3	59.2	50.2	219.9
SD	16.8	1.7	10.1	60.9	1.3	5.0	14.1	1.7	5.1	2.6	6.5	28.2
Q_2 (mg kg^{-1})	878.1	137.3	541.8	1597.0	111.5	374.3	412.3	73.5	384.7	164.6	134.7	578.9
SD	61.5	6.1	55.9	283.5	12.1	36.5	22.2	4.2	43.2	10.0	6.9	43.5
Q_1/Q_{tot} (%)	1.2	1.7	2.2	3.7	2.9	2.7	2.1	5.0	4.8	0.5	6.4	5.9
$(Q_1 + Q_2)/Q_{tot}$ (%)	4.3	14.4	14.3	12.2	17.7	19.6	3.9	16.9	15.1	1.8	23.4	21.5
λ_1 (min^{-1})	0.0755	0.0446	0.0244	0.0308	0.0358	0.0222	0.1465	0.0375	0.0410	0.1613	0.0239	0.0385
SD	0.0091	0.0082	0.0035	0.0046	0.0040	0.0027	0.0120	0.0038	0.0023	0.0327	0.0044	0.0089
λ_2 (min^{-1})	0.0012	0.0010	0.0007	0.0009	0.0007	0.0007	0.0047	0.0012	0.0007	0.0013	0.0014	0.0015
SD	0.0002	0.0001	0.0002	0.0003	0.0001	0.0001	0.0007	0.0002	0.0002	0.0002	0.0003	0.0004
$t_{1(1/2)}$ (min)	9	16	28	23	19	31	5	18	17	4	29	18
$t_{2(1/2)}$ (min)	578	693	990	770	990	990	147	578	990	533	495	462

Q_{tot} total metal content in PM_{10}, Q_1 labile pool associated to the constant λ_1 and the half-life $t_{1(1/2)}$, Q_2 less labile pool associated to the constant λ_2 and the half-life $t_{2(1/2)}$

*Span is used to assess the width of the size distribution and calculated from (D90-D10)/D50

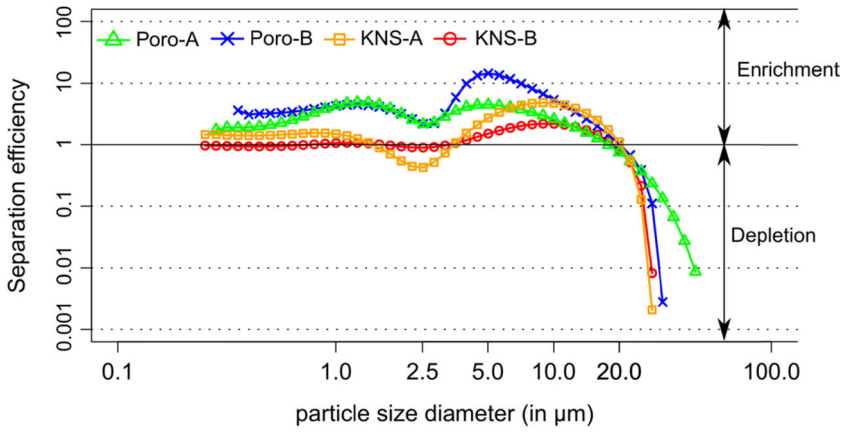

Fig. 4 Separation efficiency of the tube (L = 6 m and D = 0.04 m) as a function of particle size diameter

manner, our new device performs a narrower separation than the one presented in Goossens (2012).

The span of the $F_{<10\mu m}$ fraction was always small: 1.4–1.7 (Table 2), indicating a narrow size distribution after separation. The tube geometry was therefore appropriate to isolate the smallest particles and to produce homogeneous samples.

Kinetic extraction of the PM_{10} fraction The total contents in Ni, Co, and Mn in the PM_{10} fraction (Q_{tot} in Table 2) were similar to those of the $F_{<100\mu m}$ fraction (Table 1), and enriched in comparison with $F_{<2mm}$. The two first-order reactions used to fit kinetic extractions, as depicted in Fig. 5, were statistically validated, whatever the soil or metal: the regression estimates were significantly non null ($p < 0.05$), with R^2 values better than 0.98. The λ_1 values (0.02–0.16 min^{-1}) were one or two orders of magnitude greater than the corresponding λ_2 (0.0007–0.0047 min^{-1}). These first results obtained on weathered ultramafic soil are compatible with those from previous studies performed under similar chemical conditions, but on different types of materials: historical mining soils (Camizuli et al. 2014) and sediments (Yu and Klarup 1994; Chakraborty et al. 2014). Expressed as half-lives, 50 % of the first (labile) pool was extracted within the first 4–31 min. This time is low compared to the average time for fine particle isolation by wet techniques, which is typically 10–960 min (Ajmone-Marsan et al. 2008; Ljung et al. 2008; Madrid et al. 2008; Webber et al. 2008; Luo et al. 2011; Boisa et al. 2014). Even though wet separation techniques do not operate with a strong extractant,

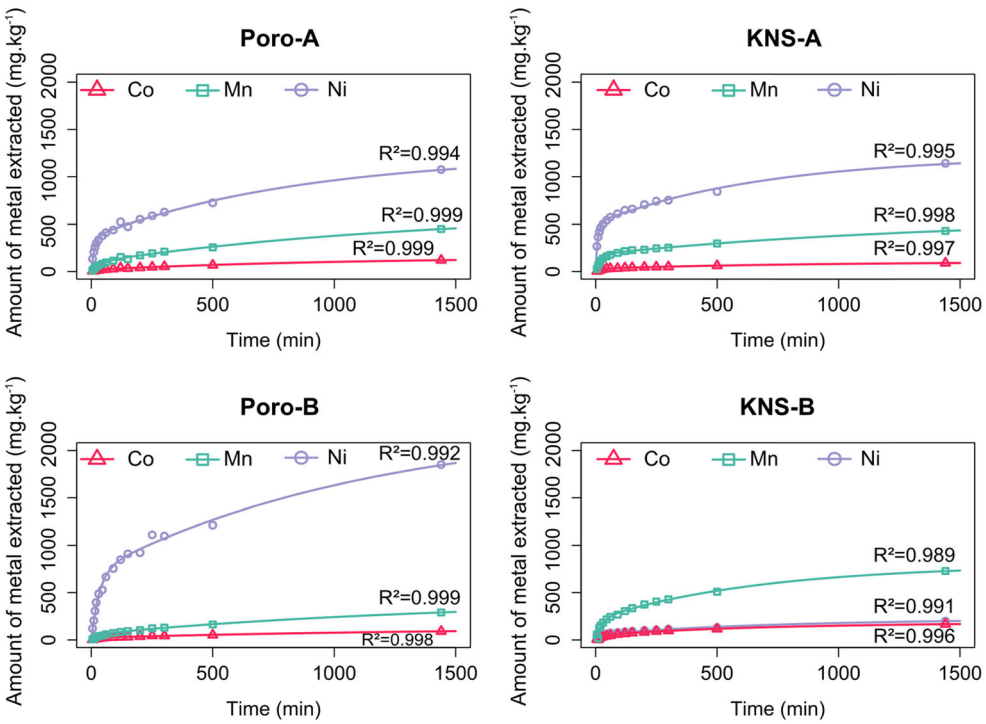

Fig. 5 Ni, Co, and Mn kinetic extractions with EDTA, performed on separated PM_{10}

such as EDTA, there is some risk of metal losses by leaching, leading to an underestimation of the bioavailable fraction, which is why dry separation techniques should be preferred.

The total amounts of the labile and less labile pools (Q_1 + Q_2) are small, compared to the total Ni, Co, and Mn contents of the PM_{10} fractions (always <20 %, Table 2), with Q_2 generally greater than Q_1. This, therefore, means that more than 80 % of Ni, Co, and Mn is not bioavailable, but strongly bound to particles. This result is in agreement with geological history, since bulk parent soils in New Caledonia were subjected to weathering for at least the past 11 Ma (Trescases 1973; Cluzel et al. 2012). A large amount of bioavailable metals must therefore have already been leached. Although it would be tempting to consider that the labile fraction is so small that it does not represent a threat for the environment (Q_1 just represents 0.5–6.4 % of Q_{tot}), it should be pointed out that these low percentages apply to extremely high Q_{tot} values. Such amounts are therefore far from negligible and should be monitored to prevent harm to the environment.

Conclusion

This study proposes a new way to separate fine particulate matter from bulk soil samples, using a tube with a gas flow. Separation of particles in the tube was modeled, according to size, weight, and fluid transport. A tube geometry of 6-m long and 0.04 m in diameter, tested on mining ferric technosoils, appears to be efficient to isolate PM_{10}. Experimental size distribution matches the theoretical model well, even if some of the smallest particles were lost during the process. The EDTA kinetic extractions on the PM_{10} collected fraction can easily be performed, because a sufficient amount of material can be collected by repeating 60-s runs, each isolating 3–5 mg. Dry separation techniques are preferable because they eliminate the risk of leaching the most labile metal fractions, which could otherwise lead to an underestimation of metal bioavailability.

Acknowledgments This work was funded by the CNRT (French National Center for Technological Research) "Nickel and its environment" (www.cnrt.nc). The French Ministry of Research is acknowledged for the PhD grant of CP. The authors thank Sebastien Breuil for preparing samples for analysis at INRA's soil analysis laboratory. The authors are grateful to Dr. X. Barthelemy from the Water Research Laboratory (UNSW, Australia) for his help with fluid mechanics. The authors wish to thank the anonymous reviewers for their comments.

References

AFNOR (2004) Evaluation de la qualité des sols Volume I: Méthodes d'analyse chimique. AFNOR, Saint Denis La Plaine

Ajmone-Marsan F, Biasioli M, Kralj T et al (2008) Metals in particle-size fractions of the soils of five European cities. Environ Pollut 152:73–81. doi:10.1016/j.envpol.2007.05.020

Baty F, Ritz C, Charles S et al (2015) A toolbox for nonlinear regression in R: the package nlstools. J Stat Softw 66:1–21

Bermond A, Ghestem J-P, Yousfi I (1998) Kinetic approach to the chemical speciation of trace metals in soils†. Analyst 123:785–789. doi:10.1039/a707776i

Bermond A, Varrault G, Sappin-Didier V, Mench M (2005) A kinetic approach to predict soil trace metal bioavailability: preliminary results. Plant Soil 275:21–29. doi:10.1007/s11104-004-7599-1

Boisa N, Entwistle J, Dean JR (2014) A new simple, low-cost approach for generation of the PM10 fraction from soil and related materials: application to human health risk assessment. Anal Chim Acta 852:97–104. doi:10.1016/j.aca.2014.09.038

Camizuli E, Monna F, Bermond A et al (2014) Impact of historical mining assessed in soils by kinetic extraction and lead isotopic ratios. Sci Total Environ 472:425–436. doi:10.1016/j.scitotenv.2013.10.103

Carvacho OF, Ashbaugh LL, Brown M, Flocchini RG (2002) Measurement of PM2.5 emission potential from soil using the UC Davis resuspension test chamber. In: ICAR5, p 88–91

Chakraborty M, Ahmad M, Singh R et al (2002) Determination of the emission rate from various opencast mining operations. Environ Model Softw 17:467–480. doi:10.1016/S1364-8152(02)00010-5

Chakraborty P, Chakraborty S, Ramteke D, Chennuri K (2014) Kinetic speciation and bioavailability of copper and nickel in mangrove sediments. Mar Pollut Bull 88:224–230. doi:10.1016/j.marpolbul.2014.08.040

Chesworth W (2008) Encyclopedia of soil science

Chow JC, Watson JG, Houck JE et al (1994) A laboratory resuspension chamber to measure fugitive dust size distributions and chemical compositions. Atmos Environ 28:3463–3481

Cluzel D, Maurizot P, Collot J, Sevin B (2012) An outline of the geology of New Caledonia; from Permian—Mesozoic southeast Gondwanaland active margin to Cenozoic obduction and supergene evolution. Episodes 35:72–86. doi:10.1029/2004TC001709

Fangueiro D, Bermond A, Santos E et al (2005) Kinetic approach to heavy metal mobilization assessment in sediments: choose of kinetic equations and models to achieve maximum information. Talanta 66:844–857. doi:10.1016/j.talanta.2004.12.036

Geagea ML, Stille P, Gauthier-Lafaye F, Millet M (2008) Tracing of industrial aerosol sources in an urban environment using Pb, Sr, and Nd isotopes. Environ Sci Technol 42:692–698

Gill TE, Zobeck TM, Stout JE, Gregory JM (1999) Fugitive dust generation in the laboratory. Proc Wind Eros Int Symp USDA-ARS Wind Eros Res Unit, Kansas State Univ, Manhattan, KS, p 1–9

Gill TE, Zobeck TM, Stout JE (2006) Technologies for laboratory generation of dust from geological materials. J Hazard Mater 132:1–13. doi:10.1016/j.jhazmat.2005.11.083

Goossens D (2012) A method for dry extracting large volumes of fine particulate matter from bulk soil samples. Air Qual Atmos Heal 5:425–431. doi:10.1007/s11869-011-0142-7

Greenwell LL, Jones TP, Richards RJ (2002) The collection of PM10 for toxicological investigation: comparisons between different collecting devices. Environ Monit Assess 79:251–273. doi:10.1023/A:1020230727359

Gutzman DW, Langford CH (1993) Kinetic study of the speciation of copper(II) bound to a hydrous ferric oxide. Environ Sci Technol 27:1388–1393. doi:10.1021/es00044a014

Harrison RM, Deacon AR, Jones MR, Appleby RS (1997) Sources and processes affection concentrations of PM10 and PM2.5 particulate matter in Birmingham (U.K.). Atmos Environ 31:4103–4117. doi:10.1016/S1352-2310(97)00296-3

Huang PM, Li Y, Sumner ME (eds) (2012) Handbook of soil sciences: properties and processes, 2 ed. CRC Press, Boca Raton, Florida

IUSS Working Group WRB (2014) World reference base for soil resources 2014

Jalali M, Tabar SS (2013) Kinetic extractions of nickel and lead from some contaminated calcareous soils. Soil Sediment Contam An Int J 22:56–71. doi:10.1080/15320383.2012.714420

Janssen NA, Hoek G, Brunekreef B et al (1998) Personal sampling of particles in adults: relation among personal, indoor, and outdoor air concentrations. Am J Epidemiol 147:537–547. doi:10.1093/oxfordjournals.aje.a009485

Järup L (2003) Hazards of heavy metal contamination. Br Med Bull 68:167–182. doi:10.1093/bmb/ldg032

Jones TP, Williamson BJ, Bérubé KA, Richards RJ (2001) Microscopy and chemistry of particles collected on TEOM filters: Swansea, South Wales, 1998-1999. Atmos Environ 35:3573–3583. doi:10.1016/S1352-2310(00)00570-7

Kampa M, Castanas E (2008) Human health effects of air pollution. Environ Pollut 151:362–367. doi:10.1016/j.envpol.2007.06.012

Labanowski J, Monna F, Bermond A et al (2008) Kinetic extractions to assess mobilization of Zn, Pb, Cu, and Cd in a metal-contaminated soil: EDTA vs. citrate. Environ Pollut 152:693–701. doi:10.1016/j.envpol.2007.06.054

Lafon S, Alfaro SC, Chevaillier S, Louis J (2014) A new generator for mineral dust aerosol production from soil samples in the laboratory: GAMEL. Aeolian Res 15:319–334. doi:10.1016/j.aeolia.2014.04.004

Latham M, Quantin P, Aubert G (1978) Etude des sols de la Nouvelle-Calédonie: nouvel essai sur la classification, la caractérisation, la pédogenèse et les aptitudes des sols de Nouvelle-Calédonie: carte pédologique de la Nouvelle-Calédonie à 1/1 000 000: carte d'aptitudes culturale et for

Ljung K, Torin A, Smirk M et al (2008) Extracting dust from soil: a simple solution to a tricky task. Sci Total Environ 407:589–593. doi:10.1016/j.scitotenv.2008.09.007

Lo IMC, Yang XY (1999) EDTA extraction of heavy metals from different soil fractions and synthetic soils. Water Air Soil Pollut 109:219–236. doi:10.1023/A:1005000520321

Losfeld G, L'Huillier L, Fogliani B et al (2015) Mining in New Caledonia: environmental stakes and restoration opportunities. Environ Sci Pollut Res 22:5592–5607. doi:10.1007/s11356-014-3358-x

Luo X, Yu S, Li X (2011) Distribution, availability, and sources of trace metals in different particle size fractions of urban soils in Hong Kong: implications for assessing the risk to human health. Environ Pollut 159:1317–1326. doi:10.1016/j.envpol.2011.01.013

Madrid F, Biasioli M, Ajmone-Marsan F (2008) Availability and bioaccessibility of metals in fine particles of some urban soils. Arch Environ Contam Toxicol 55:21–32. doi:10.1007/s00244-007-9086-1

Manouchehri N, Besançon S, Bermond A (2006) Major and trace metal extraction from soil by EDTA: equilibrium and kinetic studies. Anal Chim Acta 559:105–112. doi:10.1016/j.aca.2005.11.050

Morselli L, Olivieri P, Brusori B, Passarini F (2003) Soluble and insoluble fractions of heavy metals in wet and dry atmospheric depositions in Bologna, Italy. Environ Pollut 124:457–469. doi:10.1016/S0269-7491(03)00013-7

Peters RW (1999) Chelant extraction of heavy metals from contaminated soils. J Hazard Mater 66:151–210

Quantin P, Becquer T, Bourdon E et al (1996) Composition minéralogique et disponibilité des éléments Mn, Ni, Cr, Co et Zn de sols "ferritiques" dérivés de péridotites en Nouvelle-Calédonie. In: Journées Nationales de l'Etude des Sols: Sols et Transferts des Polluants dans les Paysages: Rennes 96, 5., Rennes (FRA), 1996/04/22–25, p 221–222

Quantin C, Becquer T, Berthelin J (2002) Mn-oxide: a major source of easily mobilisable Co and Ni under reducing conditions in New Caledonia Ferralsols. Comptes Rendus Geosci 334:273–278. doi:10.1016/S1631-0713(02)01753-4

R Development Core Team (2012) R: a language and environment for statistical computing

Ragosta M, Caggiano R, Emilio MD et al (2006) PM 10 and heavy metal measurements in an industrial area of southern Italy. Atmos Res 81:304–319. doi:10.1016/j.atmosres.2006.01.006

Sánchez de la Campa AM, De la Rosa JD, Querol X et al (2007) Geochemistry and origin of PM10 in the Huelva region, southwestern Spain. Environ Res 103:305–316. doi:10.1016/j.envres.2006.06.011

Semlali RM, van Oort F, Denaix L, Loubet M (2001) Estimating distributions of endogenous and exogenous Pb in soils by using Pb isotopic ratios. Environ Sci Technol 35:4180–4188. doi:10.1021/es0002621

Singer A, Zobeck TM, Poberezsky L, Argaman E (2003) The PM10 and PM2.5 dust generation potential of soils/sediments in the southern Aral Sea basin, Uzbekistan. J Arid Environ 54:705–728. doi:10.1006/jare.2002.1084

Sinha S, Banerjee SP (1997) Characterization of haul road dust in an Indian opencast iron ore mine. Atmos Environ 31:2809–2814. doi:10.1016/S1352-2310(97)00095-2

Tasić M, Đurić-stanojević B, Rajšić S (2006) Physico-chemical characterization of PM10 and PM2.5 in the Belgrade urban area. Acta Chim Slov 53:401–405

Trescases J-J (1973) Weathering and geochemical behaviour of the elements of ultramafic rocks in New Caledonia. Bur Miner Resour Geol Geophys Canberra 141:149–161

Webber JS, Blake DJ, Ward TJ, Pfau JC (2008) Separation and characterization of respirable amphibole fibers from Libby, Montana. Inhal Toxicol 20:733–740. doi:10.1080/08958370801932544

Wickham H (2009) ggplot2: elegant graphics for data analysis. Springer-Verlag, New York

Yu J, Klarup D (1994) Extraction kinetics of copper, zinc, iron, and manganese from contaminated sediment using disodium Ethylenediaminetetraacetate. Water Air Soil Pollut 75:205–225. doi:10.1007/BF00482938